MODIS ATMOSPHERIC PROFILE RETRIEVAL ALGORITHM THEORETICAL BASIS DOCUMENT

W. PAUL MENZEL[1] and LIAM E. GUMLEY[2]

University of Wisconsin-Madison

1225 W. Dayton St.

Madison, WI 53706

Version 4

November 30, 1998

---

1 NOAA/NESDIS (Paul.Menzel@ssec.wisc.edu)

2 Cooperative Institute for Meteorological Satellite Studies (Liam.Gumley@ssec.wisc.edu)

TABLE OF CONTENTS

1. Introduction

The purpose of this document is to present an algorithm for retrieving vertical profiles of atmospheric temperature and moisture from multi-wavelength thermal radiation measurements in clear skies. While the MODIS is not a sounding instrument, it does have many of the spectral bands found on the High resolution Infrared Radiation Sounder (HIRS) currently in service on the polar orbiting NOAA TIROS Operational Vertical Sounder (TOVS). Thus it will possible to generate profiles of temperature and moisture as well as total column estimates of precipitable water vapor, ozone, and atmospheric stability from the MODIS infrared radiance measurements. These parameters will be used to correct for atmospheric effects for some of the MODIS products (such as sea surface and land surface temperatures, ocean aerosol properties, water leaving radiances, photosynthetically active radiation) as well as to characterize the atmospheric state for global greenhouse studies. The MODIS algorithms will be adapted from the operational HIRS and GOES algorithms, with adjustments to accommodate the absence of stratospheric sounding spectral bands and to realize the advantage of greatly increased spatial resolution (1 km MODIS versus 17 km HIRS) with good radiometric signal to noise (better than 0.35 C for typical scene temperatures in all spectral bands).

In this document, we offer some background to the retrieval problem, review the MODIS instrument characteristics, describe the theoretical basis of the MODIS retrieval algorithm, discuss the practical aspects of the algorithm implementation, and outline the planned validation approach.

2. Overview and background information

The purpose of this document is to provide a description of the theoretical and practical aspects of the temperature and moisture retrieval algorithm we are developing for MODIS. Most of the sounding expertise for this endeavor has been acquired with existing infrared sounding instruments, so this document necessarily focuses on results and experience from these sensors. The techniques developed for existing sensors will, we believe, translate directly to the MODIS instrument.

2.1 *Objectives*

The objective of this work is to develop an operational algorithm for retrieving vertical profiles (soundings) of temperature and moisture, total column ozone burden, total column precipitable water vapor, and several atmospheric stability indices from clear sky radiances measured by MODIS. The methods presented here are based on the work of Smith et al. (1985), and more recent similar work by Smith and Woolf (1988) and Hayden (1988). The clear advantage of MODIS for retrieving atmospheric profiles is its combination of fifteen infrared spectral channels suitable for sounding and high spatial resolution suitable for imaging (1 km at nadir). Temperature and moisture profiles at MODIS spatial resolution are required by a number of other MODIS investigators, including those developing sea surface temperature and land surface temperature retrieval algorithms. Total ozone and precipitable water vapor estimates at MODIS resolution are required by MODIS investigators developing atmospheric correction algorithms. The combination of high spatial resolution sounding data from MODIS, and high spectral resolution sounding data from AIRS, will provide a wealth of new information on atmospheric structure in clear skies. Cloud filtering will be achieved with the aid of the cloud mask product (ATBD MOD-06).

2.2 *History*

Inference of atmospheric temperature profiles from satellite observations of thermal infrared emission was first suggested by King (1956). In this pioneering paper, King pointed out that the angular radiance (intensity) distribution is the Laplace transform of the Planck intensity distribution as a function of the optical depth, and illustrated the feasibility of deriving the temperature profile from the satellite intensity scan measurements. Kaplan (1959) advanced the temperature sounding concept by demonstrating that vertical resolution of the temperature field could be inferred from the spectral distribution of atmospheric emission. Kaplan noted that observations in the wings of a spectral band sense deeper regions of the atmosphere, whereas observations in the band center see only the very top layer of the atmosphere, since the radiation mean free path is small. Thus by properly selecting a set of sounding spectral channels at different wavelengths, the observed radiances could be used to make an interpretation of the vertical temperature distribution in the atmosphere.

Wark (1961) proposed a satellite vertical sounding program to measure atmospheric temperature profiles, and the first satellite sounding instrument (SIRS-A) was launched on NIMBUS-3 in 1969 (Wark and Hilleary, 1970). Successive experimental instruments on the NIMBUS series of polar orbiting satellites led to the development of the TIROS-N series of operational polar-orbiting satellites in 1978. These satellites introduced the TIROS Operational Vertical Sounder (TOVS, Smith et al. 1979), consisting of the High-resolution Infrared Radiation Sounder (HIRS), the Microwave Sounding Unit (MSU), and the Stratospheric Sounding Unit (SSU). This same series of instruments continues to fly today on the NOAA operational polar orbiting satellites. HIRS provides 17 km spatial resolution at nadir with 19 infrared sounding channels. The first sounding instrument in geostationary orbit was the GOES VISSR Atmospheric Sounder (VAS, Smith et al. 1981) launched in 1980. The current generation GOES-8 sounder (Menzel and Purdom, 1994) provides 8 km spatial resolution with 18 infrared sounding channels; the GOES retrieval algorithm is detailed in Ma et al. (1999). An excellent review of the history of satellite temperature and moisture profiling is provided by Smith (1991).

2.3 *Instrument Characteristics*

MODIS is a scanning spectroradiometer with 36 spectral bands between 0.645 and 14.235 μm (King et al. 1992). Table 1 summarizes the MODIS technical specifications.

Table 1: MODIS Technical Specifications

Orbit:	705 km altitude, sun-synchronous, 10:30 a.m. descending node
Scan Rate:	20.3 rpm, cross track
Swath Dimensions:	2330 km (cross track) by 10 km (along track at nadir)
Quantization:	12 bits
Spatial Resolution:	250 m (bands 1-2), 500 m (bands 3-7), 1000 m (bands 8-36)

Table 2 shows the MODIS spectral bands that will be used in our MODIS algorithm . Note that in most cases the predicted (goal) noise is expected to better than the specification. The data rate with 12 bit digitization and a 100% duty cycle is expected to be approximately 5.1×10^6 bits/sec (55 Gbytes/day).

Table 2: MODIS Spectral Band Specifications

Primary Atmospheric Application	Band	Bandwidth[1]	$T_{typical}$ (K)	Radiance[2] at $T_{typical}$	NEΔT (K) Specification	NEΔT (K) Predicted
Surface Temperature	20	3.660-3.840	300	0.45	0.05	0.05
	22	3.929-3.989	300	0.67	0.07	0.05
	23	4.020-4.080	300	0.79	0.07	0.05
Temperature profile	24	4.433-4.498	250	0.17	0.25	0.15
	25	4.482-4.549	275	0.59	0.25	0.10
Moisture profile	27	6.535-6.895	240	1.16	0.25	0.05
	28	7.175-7.475	250	2.18	0.25	0.05
	29	8.400-8.700	300	9.58	0.05	0.05
Ozone	30	9.580-9.880	250	3.69	0.25	0.05
Surface Temperature	31	10.780-11.280	300	9.55	0.05	0.05
	32	11.770-12.270	300	8.94	0.05	0.05
Temperature profile	33	13.185-13.485	260	4.52	0.25	0.15
	34	13.485-13.785	250	3.76	0.25	0.20
	35	13.785-14.085	240	3.11	0.25	0.25
	36	14.085-14.385	220	2.08	0.35	0.35

[1] μm at 50% response

[2] $W\ m^{-2}\ sr^{-1}\ \mu m^{-1}$

Figure 1 shows the spectral responses of the MODIS infrared bands in relation to an atmospheric emission spectrum computed by FASCOD3P for the US standard atmosphere.

Figure 1: MODIS infrared spectral response. Nadir viewing emission spectrum of U.S. Standard Atmosphere from FASCOD3P.

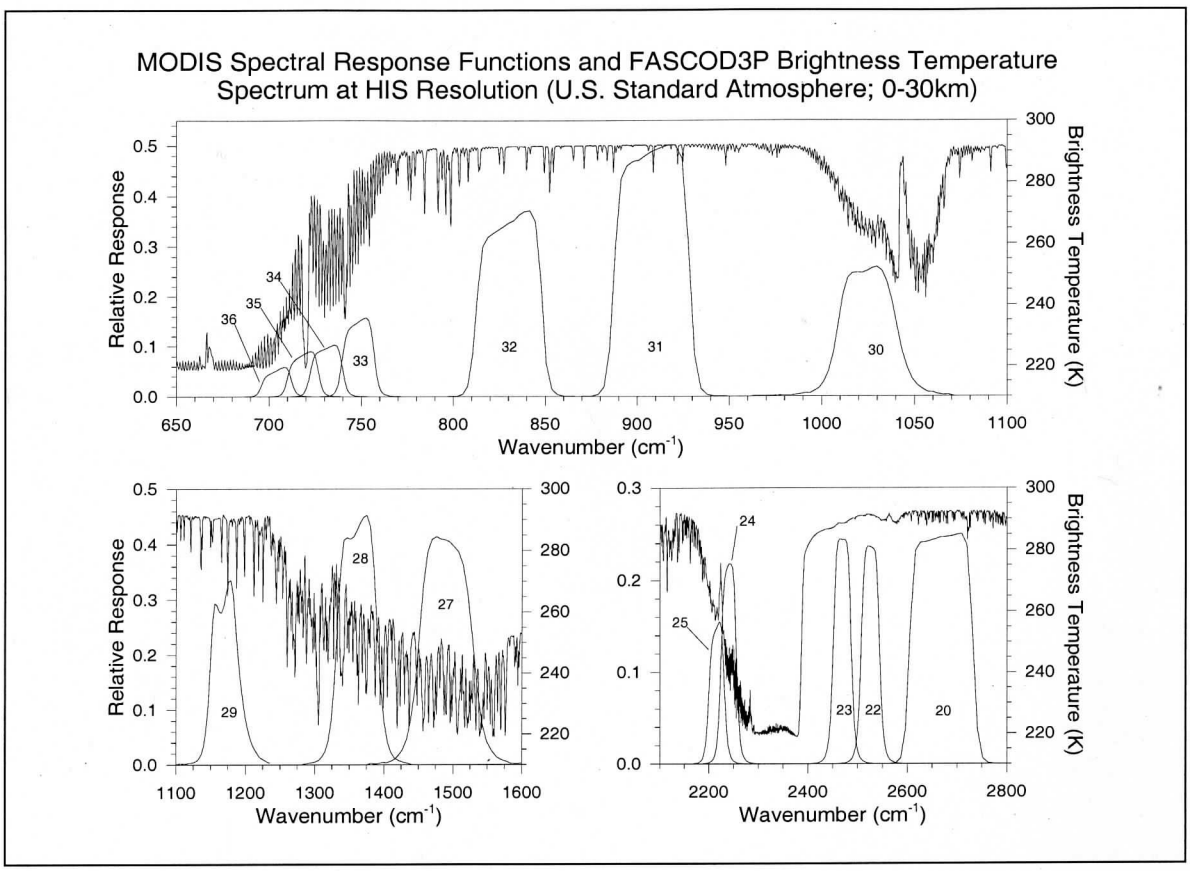

3. Algorithm Description

In section we describe the theoretical basis and practical implementation of the atmospheric profile retrieval algorithm.

3.1 *Theoretical Background*

In order for atmospheric temperature to be inferred from measurements of thermal emission, the source of emission must be a relatively abundant gas of known and uniform distribution. Otherwise, the uncertainty in the abundance of the gas will make ambiguous the determination of temperature from the measurements. There are two gases in the earth-atmosphere that are present in uniform abundance for altitudes below about 100 km, and show emission bands in the spectral regions that are convenient for measurement. Carbon dioxide, a minor constituent with a relative volume abundance of 0.003, has infrared vibrational-rotational bands. Oxygen, a major constituent with a relative volume abundance of 0.21, also satisfies the requirement of a uniform mixing ratio and has a microwave spin-rotational band. In addition, the emissivity of the earth surface in the surface sensitive spectral bands must be characterized and accounted for.

There is no unique solution for the detailed vertical profile of temperature or an absorbing constituent because (a) the outgoing radiances arise from relatively deep layers of the atmosphere, (b) the radiances observed within various spectral channels come from overlapping layers of the atmosphere and are not vertically independent of each other, and (c) measurements of outgoing radiance possess errors. As a consequence, there are a large number of analytical approaches to the profile retrieval problem. The approaches differ both in the procedure for solving the set of spectrally independent radiative transfer equations (e.g., matrix inversion, numerical iteration) and in the type of ancillary data used to constrain the solution to insure a meteorologically meaningful result (e.g., the use of atmospheric covariance statistics as opposed to the use of an a priori estimate of the profile structure). There are some excellent papers in the literature which review the retrieval theory which has been developed over the past few decades (Fleming and Smith, 1971; Fritz et al., 1972; Rodgers, 1976; Twomey, 1977; and Houghton et al. 1984). The following sections present

the mathematical basis for two of the procedures which have been utilized in the operational retrieval of atmospheric profiles from satellite measurements.

3.1.1a *Statistical Regression Profile Retrieval*

A computationally efficient method for determining temperature and moisture profiles from satellite sounding measurements uses previously determined statistical relationships between observed (or modeled) radiances and the corresponding atmospheric profiles. This method is often used to generate a first-guess for a physical retrieval algorithm, as is done in the International TOVS Processing Package (ITPP, Smith et al., 1993). The statistical regression algorithm for atmospheric temperature is described in detail in Smith et. al. (1970), and can be summarized as follows (the algorithm for moisture profiles is formulated similarly). In cloud-free skies, the radiation received at the top of the atmosphere at frequency ν is the sum of the radiance contributions from the Earth's surface and from all levels in the atmosphere,

$$R(\nu_j) = \sum_{i=1}^{N} B[\nu_j, T(p_i)] w(\nu_j, p_i) \qquad (1)$$

where

$w(\nu_j, p_i) = \varepsilon(\nu_j, p_i)\tau(\nu_j, 0 \rightarrow p_i)$ is the weighting function,

$B[\nu_j, T(p_i)]$ is the Planck radiance for pressure level i at temperature T,

$\varepsilon(\nu_j, p_i)$ is the spectral emissivity of the emitting medium at pressure level i,

$\tau(\nu_j, 0 \rightarrow p_i)$ is the spectral transmittance of the atmosphere above pressure level i.

The problem is to determine the temperature (and moisture) at N levels in the atmosphere from M radiance observations. However because the weighting functions are broad and represent an average radiance contribution from a layer, the M radiance observations are interdependent, and hence there is no unique solution. Furthermore, the solution is unstable in that small errors in the radiance observations produce large errors in the temperature profile. For this reason, the solution is approximated in a linearized form. First (1) is re-written in terms of a deviation from an initial state,

$$R(\nu_j) - R_0(\nu_j) = \sum_{i=1}^{N} \{B[\nu_j, T(p_i)] - B[\nu_j, T_0(p_i)]\} w(\nu_j, p_i) + e(\nu_j) \quad (2)$$

where

$e(\nu_j)$ is the measurement error for the radiance observation.

In order to solve (2) for the temperature profile T it is necessary to linearize the Planck function dependence on frequency. This can be achieved since in the infrared region the Planck function is much more dependent on temperature than frequency. Thus the general inverse solution of (2) for the temperature profile can be written as

$$T(p_i) - T_0(p_i) = \sum_{j=1}^{M} A(\nu_j, p_i)[R(\nu_j) - R_0(\nu_j)] \quad (3)$$

or in matrix form

$T = AR$

where $A(\nu_j, p_i)$ is a linear operator. Referring back to (2), it can be seen that in theory A is simply the inverse of the weighting function matrix. However in practice the inverse is numerically unstable.

The statistical regression algorithm seeks a "best-fit" operator matrix A that is computed using least squares methods by utilizing a large sample of atmospheric temperature and moisture soundings, and collocated radiance observations. That is, we seek to minimize the error

$$\frac{\partial}{\partial A}|AR - T|^2 = 0$$

which is solved by the normal equations to yield

$$A = (R^T R)^{-1} R^T T \quad (5)$$

where

$(R^T R)$ is the covariance of the radiance observations,

$(R^T T)$ is the covariance of the radiance observations with the temperature profile.

The radiance observations may be from actual post-launch measurements, or computed pre-launch using a temperature and moisture sounding database, and weighting functions derived from knowledge of the sensor spectral responses. The coefficients of A may be

updated as often as weekly, and different values for A are used depending on season and geographical location. In addition to the observed radiances, surface temperature and moisture estimates are used as predictors to improve the retrieval. For the at-launch version of the algorithm, these estimates will be provided by NCEP global analyses. We are currently developing a MAS regression retrieval algorithm which will provide and atmospheric profile retrieval as initial input to the surface temperature and emissivity algorithm of Zhengming Wan, and then to iterate our regression solution using their estimated surface properties as input to the iteration. This approach may be possible post-launch for MODIS.

In summary, the statistical regression algorithm has the advantage of computational speed, numerical stability, and simplicity. However it does not account for the physical properties of the Radiative Transfer Equation.

3.1.1b *Physical Profile Retrieval*

Direct physical solution of the Radiative Transfer Equation often involves several iterations between solving for the temperature and moisture profiles. They are interrelated but most solutions only solve for each one separately, assuming the other is known. Smith et al. (1985) have developed a simultaneous direct physical solution of both, and we follow this approach here. In order to solve for the temperature and moisture profiles simultaneously, a simplified form of the integral of the radiative transfer equation is considered,

$$R = B_0 + \int_0^{p_S} \tau \, dB \,,$$

which from comes integrating the atmospheric term by parts in the more familiar form of the RTE. R represents the radiance, τ the transmittance, and B the Planck radiance. Dependence on zenith angle, pressure, temperature, and frequency is assumed, but neglected in the notation for simplicity. The subscript s refers to the surface level and 0 refers to the top of the atmosphere. Then in perturbation form, where δ represents a perturbation with respect to an a priori condition

$$\delta R = \int_0^{p_S} (\partial\tau) dB + \int_0^{p_S} \tau \, d(\delta B) \,.$$

Integrating the second term on right side of the equation by parts,

$$\int_0^{p_S} \tau\, d(\delta B) = \tau\, \delta B \Big]_0^{p_s} - \int_0^{p_s} \delta B\, d\tau = \tau_s\, \delta B_s - \int_0^{p_S} \delta B\, d\tau$$

yields

$$\delta R = \int_0^{p_S} (\delta\tau) dB + \tau_s\, \delta B_s - \int_0^{p_S} \delta B\, d\tau\,.$$

Now write the differentials with respect to temperature

$$\delta R = \delta T_b \frac{\partial B}{\partial T_b}, \quad \delta B = \delta T \frac{\partial B}{\partial T}$$

and with respect to pressure

$$dB = \frac{\partial B}{\partial T}\frac{\partial T}{\partial p} dp, \quad d\tau = \frac{\partial \tau}{\partial p} dp\,.$$

Substituting this in

$$\delta T_b = \int_0^{p_S} \delta\tau \frac{\partial T}{\partial p}\left[\frac{\partial B}{\partial T} \Big/ \frac{\partial B}{\partial T_b}\right] dp - \int_0^{p_S} \delta T \frac{\partial \tau}{\partial p}\left[\frac{\partial B}{\partial T} \Big/ \frac{\partial B}{\partial T_b}\right] dp + \delta T_s \left[\frac{\partial B_s}{\partial T_s} \Big/ \frac{\partial B}{\partial T_b}\right] \tau_s$$

where T_b is the brightness temperature. Finally, assume that the transmittance perturbation is dependent only on the uncertainty in the column of precipitable water density weighted path length u according to the relation

$$\delta\tau = \frac{\partial \tau}{\partial u} \delta u$$

Thus

$$\begin{aligned} \delta T_b &= \int_0^{p_S} \delta u \frac{\partial T}{\partial p}\frac{\partial \tau}{\partial u}\left[\frac{\partial B}{\partial T} \Big/ \frac{\partial B}{\partial T_b}\right] dp - \int_0^{p_S} \delta T \frac{\partial \tau}{\partial p}\left[\frac{\partial B}{\partial T} \Big/ \frac{\partial B}{\partial T_b}\right] dp + \delta T_s \left[\frac{\partial B_s}{\partial T_s} \Big/ \frac{\partial B}{\partial T_b}\right] \tau_s \\ &= f\left[\delta u, \delta T, \delta T_s\right] \end{aligned}$$

where f represents some function.

The perturbations are with respect to some a priori condition which may be estimated from climatology, regression, or more commonly from an analysis or forecast provided by a numerical model. In order to solve for δu, δT, and δT_S from a set spectrally independent radiance observations δT_b, the perturbation profiles are represented in terms of arbitrary basis functions $\phi(p)$; so

$$\delta T_s = \alpha_0 \phi_0$$

$$\delta u(p) = \sum_{i=1}^{Q} \alpha_i \int_0^p q(p)\phi_i(p)dp$$

where the water vapor mixing ratio is given by $q(p) = g\ \partial u/\partial p$ and $\delta q = g \sum \alpha q \phi$

$$\delta T(p) = -\sum_{i=Q+1}^{L} \alpha_i \phi_i(p).$$

Then for M spectral channel observations

$$\delta T_{bj} = \sum_{i=0}^{L} \alpha_i \psi_{ij} \qquad \text{where } j = 1,...,M$$

and

$$\psi_{0j} = \left[\frac{\partial B_j}{\partial T_s} \Big/ \frac{\partial B_j}{\partial T_{bj}}\right] \tau_{sj},$$

$$\psi_{ij} = \int_0^{p_s} \left[\int_0^p q\,\phi_i\,dp\right] \left[\frac{\partial T}{\partial p}\frac{\partial \tau_j}{\partial u}\right] \left[\frac{\partial B_j}{\partial T} \Big/ \frac{\partial B_j}{\partial T_{bj}}\right] dp, \qquad i = 1,...,Q$$

$$\psi_{ij} = \int_0^{p_s} \phi_i \frac{\partial \tau_j}{\partial p} \left[\frac{\partial B_j}{\partial T} \Big/ \frac{\partial B_j}{\partial T_{bj}}\right] dp, \qquad i = Q+1,...,L$$

or in matrix form

$$t_b = \psi \alpha.$$

A least squares solution suggests that

$$\alpha = \left(\psi^t \psi\right)^{-1} \psi^t t_b \approx \left(\psi^t \psi + \gamma I\right)^{-1} \psi^t t_b$$

where the Lagrangian multiplier γ is incorporated to stabilize the matrix inverse.

There are many reasonable choices for the pressure basis functions $\phi(p)$. For example empirical orthogonal functions (eigenvectors of the water vapor and temperature profile covariance matrices) can be used in order to include statistical information in the solution. Also the profile weighting functions of the radiative transfer equation can be used, as can Gaussian functions that peak in different layers of the atmosphere. We intend to use the transmittance profile weighting functions as the basis functions in the MODIS temperature and moisture profile retrieval algorithm. Examples of these functions are shown in Figure 2.

Ancillary information, such as surface observations, are readily incorporated into the profile solutions as additional equations (M+2 equations to solve L unknowns).

$$q_0 - q(p_s) = g\sum_{i=1}^{Q} \alpha_i\, q(p_s)\phi_i(p_s)$$

$$T_0 - T(p_s) = -\sum_{i=Q+1}^{L} \alpha_i\, \phi_i(p_s)$$

In summary we have the following characteristics (a) the RTE is in perturbation form, (b) δT and δU are expressed as linear expansions of basis functions (empirical orthogonal functions or weighting functions), (c) ancillary observations are used as extra equations, (d) a least squares solution is sought, and (e) a simultaneous temperature and moisture profile solution produces improved moisture determinations.

Figure 2: MODIS temperature (left) and moisture (right) normalized retrieval weighting functions ($\partial\tau/\partial \ln p$) for the U.S. Standard Atmosphere at nadir view from FASCOD3P.

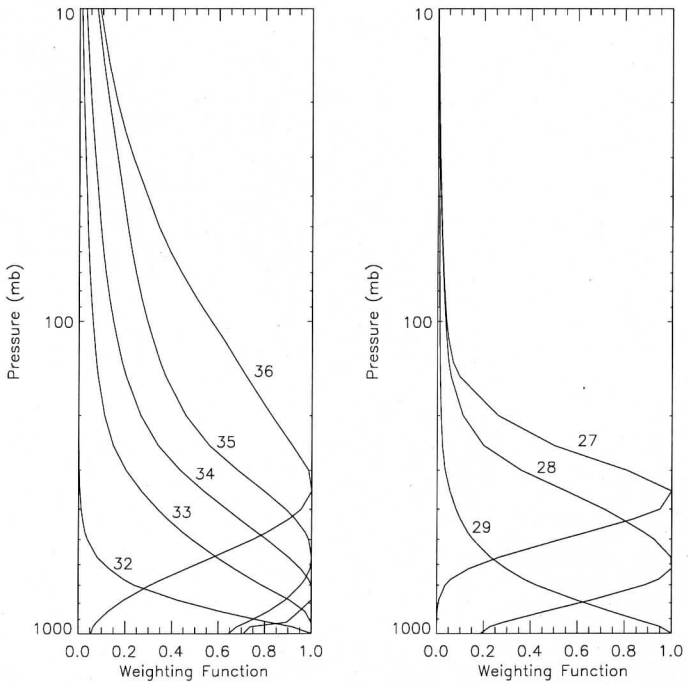

The simultaneous solution addresses the interdependence of water vapor radiance upon temperature and carbon dioxide channel radiance upon water vapor concentration. The dependence of the radiance observations on the surface emissions is accounted for by the inclusion of surface temperature as an unknown. Our experience has shown that a single matrix solution is more computationally efficient than an iterative calculation.

Sullivan et al. (1993) present results from a physical HIRS retrieval algorithm, and show global RMS differences between HIRS retrieved and collocated radiosonde measured temperature profiles of ≈ 1.9 C between 700 and 300 hPa. At the tropopause and near the Earth surface these values increase by ≈ 0.5-1.0 C. In cloudy conditions, another degree of separation between HIRS profile retrieval and radiosonde observations is found. Differences should not be interpreted literally as retrieval error; space and time discrepancies between the two types of observations contribute significantly as does atmospheric variability.

In the absence of any spectral bands sensitive to the stratosphere (bands with center wavelengths from 14.5 to 15.0 μm), the profile retrievals from the MODIS will rely on the global numerical forecast models (such as the NCEP Global Data Assimilation System, GDAS) for this information. Since the stratosphere is largely stable and slowly varying, the model should be very representative of the stratospheric conditions and the accuracy of the MODIS temperature and moisture profiles should not be significantly affected. Because MODIS has significantly higher spatial resolution (1 km MODIS versus 17 km HIRS at nadir) and maintains good signal to noise, clear sky radiance determinations will be more accurate and the retrieval coverage and accuracy is expected to be enhanced with respect to that reported in the preceding paragraph for HIRS (how much better remains to be seen from actual data). Figure 3 shows HIRS physical and statistical retrievals of the 500 hPa temperature field. Good agreement is noted.

Figure 3: NOAA-12 95/05/15 1210-1214 UTC 500 hPa temperature (degrees C).

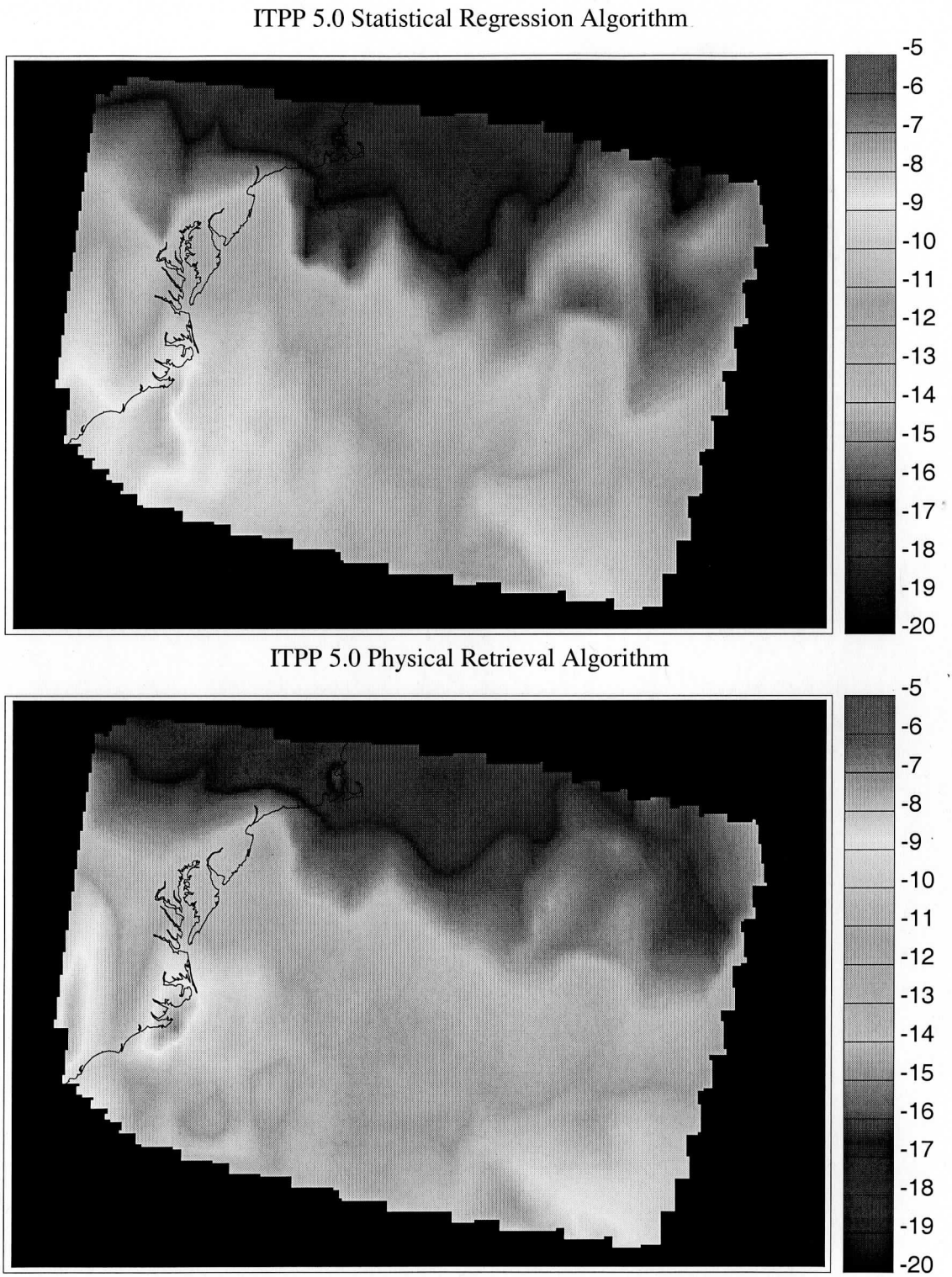

The retrieval of atmospheric profiles has been validated against radiosondes launched from land surfaces; thus it can be inferred that the retrieval is usually not significantly hindered by surface emissivity effects. There are several reasons for this. Foremost is the fact that the infrared window radiance provides a very good estimate of the effective radiating temperature, T_{eff}, for the surface (where $B(T_{eff}) = \varepsilon_{sfc}\ B(T_{sfc})$). This can be used to infer the surface contribution of the radiative transfer equation for the infrared sounding bands since the surface emissivity remains roughly the same in the longwave part of the infrared spectrum (the earth surface behaves like a gray body for the longwave infrared sounding bands). Additionally, much of the retrieval skill between 300 and 850 hPa comes from infrared spectral bands that are not very sensitive to radiation from the earth surface and receive only a small fraction of their sensed radiation from the surface.

However, improvements to the accuracy of the temperature and moisture profiles are possible with a proper accounting for the surface infrared emissivity characteristics. Plokhenko and Menzel (1999) have shown that it is possible to retrieve shortwave and longwave emissivities along with temperature and moisture profiles in a physical solution using a hemispherical directional effective emissivity model. In surface and profile retrieval calculations with MODIS Airborne Simulator data, their infrared surface emissivity solutions are strongly correlated with vegetation indices inferred from visible data. In addition the atmospheric variations of temperature and moisture were smoother and more physical (Figure 4a). While total column distributions of moisture were not significantly affected, low level mixing ratios (below 850 hPa) were sometimes adjusted by as much as 1 g/kg (Figure 4b). The MODIS Atmospheric Profiles ATBD will be updated to indicate subsequent progress in this work.

Figure 4a: Temperature and mixing ratio profile statistics (mean and standard deviation of first guess adjustment, retrieval minus guess) for the two models (with and without surface reflection).

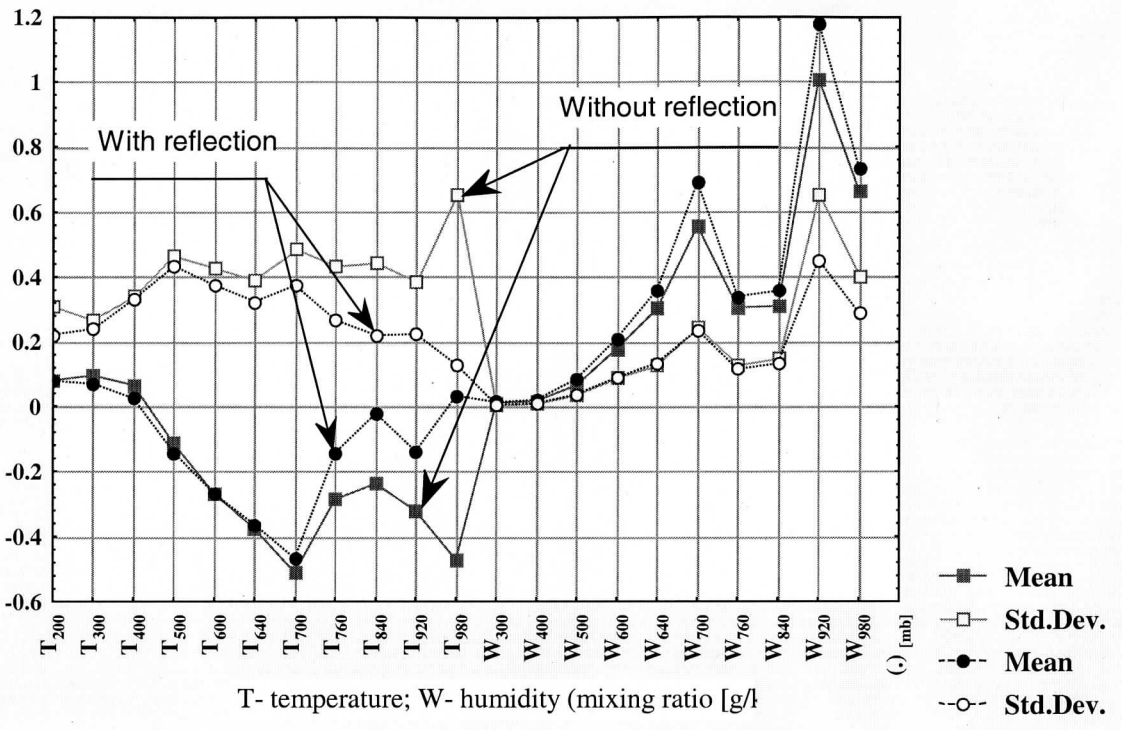

Figure 4b: Stability of the solution for the two algorithms (with and without surface reflection) as measured by the standard deviation of the second derivative of the horizontal variation of temperature or mixing ratio at a given level of the atmosphere. Smaller values are more stable and hence better depicting the actual atmospheric state.

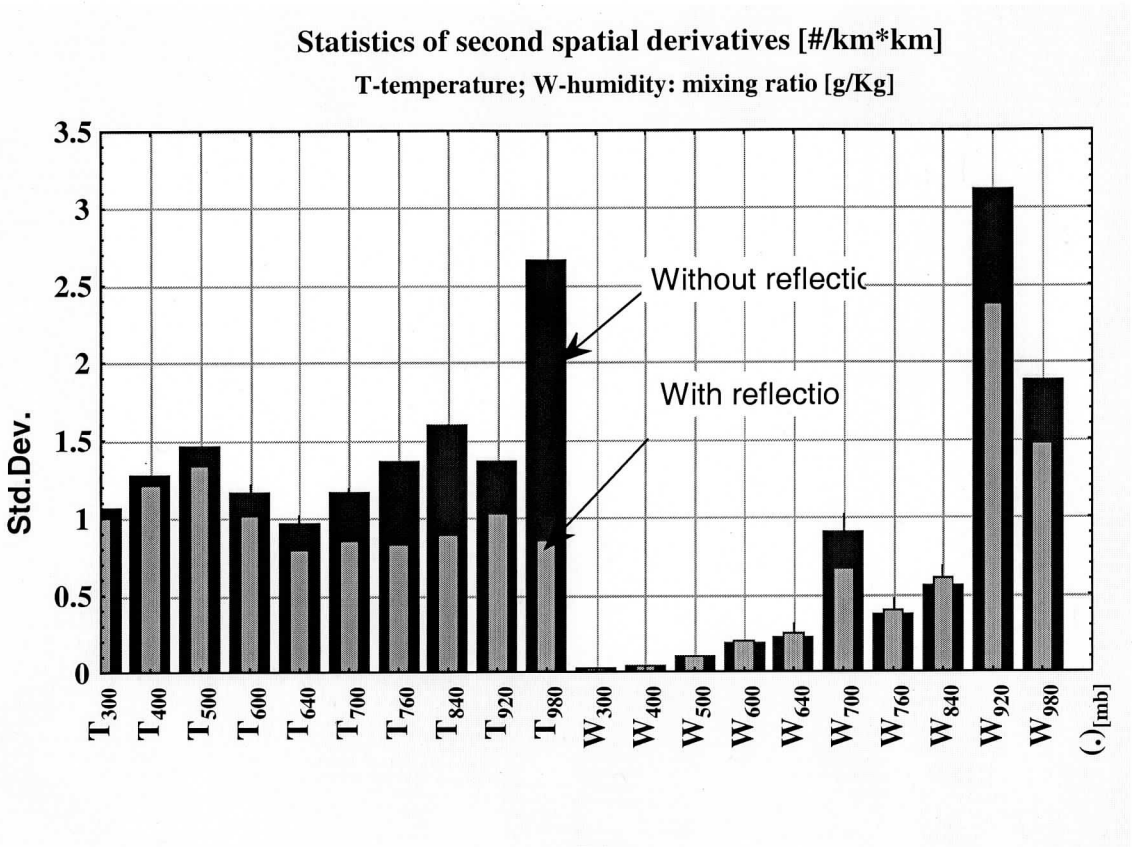

3.1.2 *Total Column Ozone*

Ozone is an important atmospheric constituent found in the atmosphere between 10 and 50 km above the earth's surface. Because it absorbs ultraviolet rays from the sun, ozone protects man from the harmful effects of ultraviolet radiation. Also, ozone is a prime source of thermal energy in the low stratosphere and has been shown to be a useful tracer for stratospheric circulation. Prabhakara et al. (1970) have exploited remote sensing of the total ozone using satellite infrared emission measurements and their studies reveal a strong correlation between the meridional gradient of total ozone and the wind velocity at tropopause levels. Shapiro et al. (1982) have indicated a possibility to predict the position and intensity of jet streams using total ozone measured by satellite.

Ma et al. (1984) described a method for obtaining total ozone with high spatial resolution from the NOAA series of satellites. The ozone concentration is mapped with the 9.6 μm ozone radiance observations obtained by HIRS. The influence of clouds must be screened out to produce reliable ozone determinations.

Ozone concentration is related to radiance to space through the transmittance $\tau(p)$. The total column ozone can be estimated from 9.6 μm radiance measurements that are comprised of contributions from stratospheric ozone amount and temperature as well as surface temperature and boundary layer water vapor. Assuming that the temperature profile and the surface temperature is well known for a given FOV, then the perturbation form of the radiative transfer equation reduces to

$$\delta T_{oz} = \int_0^{p_s} \delta\tau \frac{\partial T}{\partial p}\left[\frac{\partial B}{\partial T}\Big/\frac{\partial B}{\partial T_{oz}}\right]dp$$

where T_{OZ} is the 9.6 μm brightness temperature. Finally, assume that the transmittance perturbation is dependent only on the uncertainty in the column of ozone density weighted path length v according to the relation

$$\delta\tau = \frac{\delta T}{\partial v}\delta v$$

Thus

$$\delta T_{oz} = \int_0^{p_s} \delta v \frac{\partial T}{\partial p} \frac{\partial \tau}{\partial v} \left[\frac{\partial B}{\partial T} \Big/ \frac{\partial B}{\partial T_{oz}} \right] dp$$
$$= f[\delta v]$$

where f represents some function.

As in the profile retrieval, the perturbations are with respect to some a priori condition that may be estimated from climatology, regression, or more commonly from an analysis or forecast provided by a numerical model. In order to solve for δv from the 9.6 μm radiance observations δT_{OZ}, the perturbation profile is represented in terms of the 9.6 μm weighting function (used as the basis function $\phi(p)$); so

$$\delta v = \alpha \phi$$

where α is computed from the initial guess.

The profile shape and the vertical position of the peak ozone mixing ratio corresponding to the ozone guess profile is crucial to obtaining a satisfactory retrieval since only one ozone channel radiance in the 9.6 μm band is used. This is because the true ozone profile is assumed to have the same shape as the first guess. Therefore, to make the ozone guess profile sufficiently accurate in both shape and position of the ozone peak mixing ratio, adjustments to the vertical position and amplitude of the guess peak mixing ratio are made based on the difference between the observed brightness temperature and the calculated brightness temperature using the ozone guess profile. Specifically the vertical position is adjusted by

$$Dp = a + b\left(T_{oz}^{\ cal} - T_{oz}^{\ obs}\right)$$

where a and b are dependent on latitude and are obtained from linear regression in an independent set of conventional sounding data.

Li et al. (1999) have developed a statistical regression for total atmospheric ozone using GOES radiances ($14.7\,\mu m$, $14.4\,\mu m$, $14.1\,\mu m$, $13.6\,\mu m$ and $9.7\,\mu m$) followed by a physical iterative retrieval using only the 9.7 μm radiance. Their total ozone retrieval procedure follows the operational processing of atmospheric temperature and moisture profiles from GOES sounder measurements (Ma et al., 1999). The GOES temperature and moisture profile retrievals are used in the GOES $9.7\,\mu m$ radiative transfer calculations. The Minimum Information (MI) and Discrepancy Principle (DP) (Li and Huang 1998) comprise the

algorithm for retrieving total atmospheric ozone. Since the retrieval problem is ill-posed, a-priori information is needed to constrain the solution. A first guess ozone profile serves this purpose. The ozone first guess is generated via a regression equation in which GOES channel 1 (14.7 μm), 2 (14.4 μm), 3 (14.1 μm), 4 (13.6 μm) and 9 (9.7 μm) radiances, as well as the satellite local zenith angle and the surface pressure, are used as predictors. Since only one channel's radiance (ch. 9) contains information concerning atmospheric ozone absorption, it is difficult to modify the vertical structure of the guess ozone profile. They assume the unknown ozone profile has the following relationship with that of the first guess ozone profile:

$$X(p) = \dot{\alpha} X^0(p),$$

where $X^0(p)$ is the first guess ozone profile at pressure p (derived from the regression equation), and $X(p)$ is the ozone profile to be retrieved. According to the minimum variance inverse technique (Rodgers 1976), one can define a cost function

$$J(\alpha) = \frac{[Y^m - Y(\alpha)]^2}{\varepsilon^2} + \frac{[\alpha - \alpha^0]^2}{\sigma^2},$$

where Y^m is the satellite-observed 9.7 μm brightness temperature, $Y(\alpha)$ is the brightness temperature calculated from the unknown ozone profile $X(p)$, $\alpha^0 = 1$ is the first guess of α, ε is the observational error of the GOES 9.7 μm channel, which includes the estimated forward model error, and σ is the error of the first guess α^0. After minimizing this cost function,

$$\alpha = \alpha^0 + [\frac{Y'^2(\alpha^0)}{\varepsilon^2} + \frac{1}{\sigma^2}]^{-1} \cdot \frac{Y'^{-1}(\alpha^0)}{\varepsilon^2} \cdot [Y^m - Y(\alpha^0)],$$

where $Y'(\alpha) = \partial Y / \partial \alpha$. Therefore, α can be solved by using an iterative form of the equation. However, it is difficult to estimate the first guess noise σ^2. Usually, $\gamma^{-1} I$ is used instead of σ^2, where γ is a smoothing factor used to condition the solution, and I is the identity matrix (here $I = 1$). At this point:

$$\alpha = \alpha^0 + [\frac{Y'^2(\alpha^0)}{\varepsilon^2} + \gamma I]^{-1} \cdot \frac{Y'^{-1}(\alpha^0)}{\varepsilon^2} \cdot [Y^m - Y(\alpha^0)].$$

This is known as the minimum information solution. Since the solution is related to γ, if γ is too large, the solution will be over-constrained, and large biases could be created in the retrieval. On the other hand, if γ is too small, the solution will be less constrained, and an unstable solution will be obtained. Following Li and Huang (1998), the Discrepancy Principle is used to determine the smoothing factor γ according to

$$[Y^m - Y(\alpha(\gamma))]^2 = \varepsilon^2 .$$

Therefore, α and γ can be solved by simultaneous solution of these last two equations.

Comparisons of the GOES retrieved ozone values with Total Ozone Mapping Spectrometer (TOMS) ozone measurements from the Earth Probe (EP) satellite have been encouraging (Figure 5); the total ozone concentration can be retrieved with an accuracy better than 10% and the GOES retrievals are able to capture the main structure of the ozone distribution. This algorithm will need to be modified for MODIS application, as the 14.7 and 14.4 μm channels are missing.

Figure 5. Comparison between TOMS daily and GOES instantaneous total ozone.

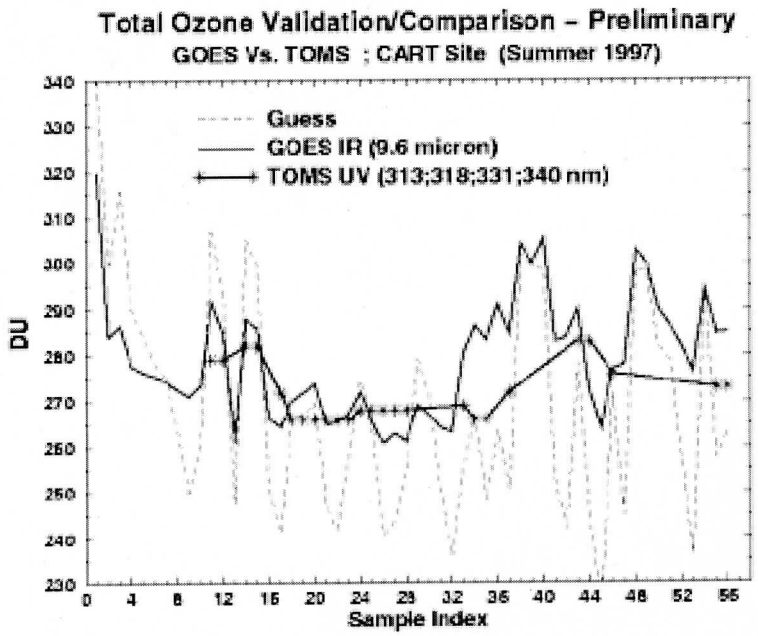

The NOAA operational HIRS algorithm offers another approach for estimating total atmospheric column ozone. Total ozone is separated into upper and lower stratospheric contributions. Warm ozone in the upper stratosphere would be estimated directly from the model first guess; cold ozone in the lower stratosphere is estimated directly from its effect on the 9.6 μm channel radiance. Determination of lower stratospheric ozone requires an estimate of foreground temperature T_f and background temperature T_b. T_f is estimated from the model first guess 50 mb temperature. T_b is estimated from the infrared window brightness temperature in the absence of any ozone. The effects of upper stratospheric ozone are removed from the 9.6 μm radiance value by the following extrapolation

$$R'_{oz} = \left[R_{oz} - A_u R(30mb)\right] / \left[1 - A_u\right]$$

where from the model first guess we calculate

$$A_u = 0.18\sqrt{E_{su}},$$
$$E_{su} = E_q(lat) + S_w,$$
$$E_q = 0.9 + 1.1\cos(lat),$$
$$S_w = D_T\left[1 + D_T(2 + D_T)\right][270 + lat]/9000,$$
$$D_T = L_R W_A / 40,$$
$$L_R = T(60mb) - T(100mb) - 1 \quad = tropospheric\ lapse\ rate,$$
$$W_A = 2T(60mb) - T(30mb) - 205 \quad = lower\ stratospheric\ temperature\ anomaly.$$

Then

$$R'_{oz} = \tau_{ls} R_b + (1 - \tau_{ls}) R_f$$

where τ_{ls} is the transmittance through the lower stratosphere, R_b is the radiance from the background, and R_f is the radiance from the foreground. Solving for τ_{ls} yields the amount of total ozone by inverting Beer's law.

It is not known yet which algorithm will perform better with MODIS data, where the stratospheric temperatures are not measured. All three (Ma, Li, and NOAA operational) are currently under investigation.

3.1.3 *Total column precipitable water vapor*

Determination of the total column precipitable water vapor is most directly done by integrating the moisture profile through the atmospheric column. However several other simpler approaches are also viable. They are briefly described below.

The split window method can be used to specify total water vapor concentration from clear sky 11 μm and 12 μm brightness temperature measurements. The water vapor is evaluated by observing the area of interest in both infrared window channels. In the atmospheric window regions the absorption is weak so that

$$\tau_w = e^{-K_w u} \approx 1 - K_w u$$

where w denotes the window channel wavelength. Thus

$$d\tau_w = -K_w\, du$$

What little absorption exists is due to water vapor, therefore, u is a measure of precipitable water vapor. The measured radiance in the window region can be written from the RTE

$$R_w = B_{sw}\left(1 - K_w u_s\right) + K_w \int_0^{u_s} B_w\, du$$

where s denotes surface, and u_s represents the total atmospheric column absorption path length due to water vapor. Defining an atmospheric mean Planck radiance

$$\overline{B}_w = \int_0^{u_s} B_w\, du \Big/ \int_0^{u_s} du$$

then

$$R_w = B_{sw}\left(1 - K_{wu_s}\right) + K_w u_s \overline{B}_w$$

Since B_{sw} is close to both R_w and B_w, first order Taylor expansion about the surface temperature T_s allows us to linearize the RTE with respect to temperature, so

$$T_{bw} = T_s\left(1 - K_w u_s\right) + K_w u_s \overline{T}_w$$

where $\overline{T}_w$ is the mean atmospheric temperature corresponding to B_w. This implies that

$$u_s = \left[T_{bw} - T_s\right] \Big/ \left[K_w\left(\overline{T}_w - T_s\right)\right]$$

Obviously, the accuracy of the determination of the total water vapor concentration depends upon the contrast between the surface temperature and the effective temperature of the atmosphere. In an isothermal situation, the total precipitable water vapor concentration is indeterminate. For two window channel wavelengths (11 and 12 μm) the split window approximation allows us to write

$$T_s = \left[K_{w2}T_{bw1} - K_{w1}T_{bw2}\right] / \left[K_{w2} - K_{w1}\right]$$

and if we express T_w as proportional to T_s

$$\overline{T}_w = a_w T_s$$

then a solution for u_s follows:

$$u_s = \frac{T_{bw2} - T_{bw1}}{(a_{w1} - 1)(K_{w2}T_{bw1} - K_{w1}T_{bw2})}$$
$$= \frac{T_{bw2} - T_{bw1}}{b_1 T_{bw1} - b_2 T_{bw2}}$$

The coefficients b_1 and b_2 can be evaluated in a linear regression analysis from prescribed temperature and water vapor profile conditions coincident with in situ observations of u_s. The weakness of the method is due to the time and spatial variability of a_w and the insensitivity of a stable lower atmospheric state when $T_{bw1} \sim T_{bw2}$ to the total precipitable water vapor concentration.

Another approach lies in the Split Window Variance Ratio, which starts from atmospheric windows with minimal moisture absorption

$$R_w = B_{sw}(1 - K_w u_s) + K_w u_s \overline{B}_w$$

Consider neighboring fields of view and assume that the air temperature is invariant, then the gradients can be written

$$DR_w = DB_{sw}(1 - K_w u_s)$$

where D indicates the differences due to different surface temperatures in the two FOVs. Convert to brightness temperatures with a Taylor expansion with respect to one of the surface temperatures, so that

$$\left[R_w(FOV1) - R_w(FOV2)\right] = \left[B_{sw}(FOV1) - B_{sw}(FOV2)\right]\left[1 - K_w u_s\right]$$
$$\left[T_w(FOV1) - T_w(FOV2)\right] = \left[T_s(FOV1) - T_s(FOV2)\right]\left[1 - K_w u_s\right]$$

Using the split windows we can arrive at an estimate for u_s in the following way. Write the ratio

$$\frac{1-K_{w1}u_s}{1-K_{w2}u_s} = \frac{dR_{w1}dB_{sw2}}{dR_{w2}dB_{sw1}}$$
$$= \frac{\left[R_{w1}(FOV1)-R_{w1}(FOV2)\right]\left[B_{sw2}(FOV1)-B_{sw2}(FOV2)\right]}{\left[R_{w2}(FOV1)-R_{w2}(FOV2)\right]\left[B_{sw1}(FOV1)-B_{sw1}(FOV2)\right]}$$
$$= \frac{\left[T_{w1}(FOV1)-T_{w1}(FOV2)\right]\left[T_s(FOV1)-T_s(FOV2)\right]}{\left[T_{w2}(FOV1)-T_{w2}(FOV2)\right]\left[T_s(FOV1)-T_s(FOV2)\right]}$$
$$= \frac{\left[T_{w1}(FOV1)-T_{w1}(FOV2)\right]}{\left[T_{w2}(FOV1)-T_{w2}(FOV2)\right]}$$

since the surface temperature cancels out. Therefore

$$\frac{1-K_{w1}u_s}{1-K_{w2}u_s} = \frac{DT_{w1}}{DT_{w2}}$$

or

$$u_s = (1-D_{12})/(K_{w1}-K_{w2}D_{12})$$

where D_{12} represents the ratio of the deviations of the split window brightness temperatures. The deviation is often determined from the square root of the variance.

The assumption in this technique is that the difference in the brightness temperatures from one FOV to the next is due only to the different surface temperatures. It is best applied to an instrument with relatively good spatial resolution, so that sufficient samples can be found in an area with small atmospheric variations and measurable surface variations in order to determine the variance of the brightness temperatures accurately. The technique was suggested by the work of Chesters et al (1983) and Kleespies and McMillin (1984); Jedlovec (1987) successfully applied it to aircraft data with 50 m spatial resolution to depict mesoscale moisture variations preceding thunderstorm development.

The experience with GOES has been that total precipitable water vapor can be retrieved with an accuracy of 10% with respect to determination from radiosondes (Menzel et al., 1998). Again not all of this difference should be construed as error but as a reflection on the differences of observation (point measurement versus area average) and differences of location in space and time.

3.1.4 *Atmospheric Stability*

One measure of the thermodynamic stability of the atmosphere is the total-totals index, defined by

$$TT = T_{850} + TD_{850} - 2\,T_{500}$$

where T_{850} and T_{500} are the temperatures at the 850 mb and 500 mb levels, respectively, and TD_{850} is the 850-mb level dew point. *TT* is traditionally estimated from radiosonde point values. For a warm moist atmosphere underlying cold mid-tropospheric air, *TT* is high (e.g., 50-60 K) and intense convection can be expected. There are two limitations of radiosonde derived *TT*: (a) the spacing of the data is too large to isolate local regions of probable convection and (b) the data are not timely since they are available only twice per day.

If we define the dew point depression at 850 mb, $D_{850} = T_{850} - TD_{850}$, then

$$TT = 2\left(T_{850} - T_{500}\right) - D_{850}$$

Although point values of temperature and dew point cannot be observed by satellite, the layer quantities observed can be used to estimate the temperature lapse rate of the lower troposphere (T_{850} - T_{500}) and the low level relative moisture concentration D_{850}. Assuming a constant lapse rate of temperature between the 850 and 200 mb pressure levels and also assuming that the dew point depression is proportional to the logarithm of relative humidity, it can be shown from the hydrostatic equation that

$$TT = 0.1489\,DZ_{850-500} - 0.0546\,DZ_{850-200} + 16.03\ln\left(RH\right)$$

where *DZ* is the geopotential thickness in meters and *RH* is the lower tropospheric relative humidity, both estimated from the MODIS radiance measurements as explained earlier.

Smith and Zhou (1982) reported several case studies using this approach. They found general agreement in gradients in space and time, with the satellite data providing much more spatial detail than the sparse radiosonde observations.

Another estimate of atmospheric stability is the lifted index, which can be derived from the MODIS determined temperature and moisture profile. The lifted index is the difference of the measured 500 mb temperature and the temperature calculated by lifting a surface parcel dry adiabatically to its local condensation level and then moist adiabatically to 500 mb. As this value goes negative it indicates increased atmospheric instability.

3.1.5 *Estimate of Errors*

A complete error analysis including the effects of instrument calibration and noise as well as ancillary input data errors remains to be completed. The past performance of these algorithms with HIRS data is documented as temperature profiles errors at about 1.9 C, dewpoint temperature profile errors at about 4 C, total column ozone at about 10%, total column water vapor at about 10%, and gradients in atmospheric stability within 0.5 C.

The profile and total atmospheric column algorithms are based on HIRS experience. One significant difference between MODIS and HIRS is the absence of any stratospheric channels on MODIS (15.0, 14.7, and 14.5 μm). This will primarily affect the accuracy of the total ozone concentration estimates. The assumption for the MODIS algorithms presented here is that the slowly varying stratospheric temperatures are estimated very well by the forecast model. The higher spatial resolution of the MODIS compared to the HIRS will make clear sky radiance estimates more accurate and hence the RMS errors of the profile retrievals can be expected to improve (possibly by 0.5 C but exactly how much remains to be seen from actual data).

3.2 *Practical Considerations*

The MODIS infrared CO_2 and H_2O channels will be used to investigate the clear sky atmosphere at 5×5 pixel resolution and to generate a global census of atmospheric stability and total precipitable water and total ozone at 5×5 pixel resolution.

3.2.1 *Radiance Biases and Numerical Considerations*

The MODIS measured radiances will have biases with respect to the forward calculated radiances using model estimates of the temperature and moisture profile for a given field of view. There are several possible causes for this bias: these include calibration errors, spectral response uncertainty, undetected cloud in the FOV, and model uncertainty. The physical retrieval method uses measured and calculated radiances (using the first guess) and thus requires that this bias be minimized. Techniques developed at the European Centre for Medium range Weather Forecast to characterize the HIRS radiance bias with respect to the ECMWF model (Eyre, 1992) will be employed in the MODIS atmospheric profile algorithm.

The transmittance model will be developed using the methods outlined by Eyre and Woolf (1988), using PLOD (Hannon et al., 1996) as the fast transmittance code.

3.2.2 *Data Processing Considerations*

Processing will be accomplished globally at 5×5 pixel resolution in regions where a sufficient number of clear FOVs are available (the threshold number of clear FOVs will be determined when instrument noise equivalent radiances are estimated in vacuum test). Clear FOVs will be averaged to reduce instrument single sample noise.

An estimate of the processing requirements for this algorithm follows. Timing tests were conducted on a Silicon Graphics Power Indigo^2 (R8000/75 Mhz). The Version 1 MODIS atmospheric profiles code (statistical regression only) was run on simulated cloud-free MODIS Level 1B radiance data supplied by the MODIS Science Data Support Team. The input dataset contained 100 MODIS scans, which translates to 1000 along track 1 kilometer pixels. Processing was done on 5×5 blocks of pixels, and input data included the Level 1B radiances, corresponding geolocation data, simulated cloud mask data, and ancillary data (surface temperature and water vapor mixing ratio). The timing shown below reflects all phases of the processing, including opening and reading input data files, computing retrieval parameters, and writing the output data file. Timing was measured using the Unix 'timex' command. Results are shown in Table 3.

Table 3: Timing test results for MODIS atmospheric profiles code (statistical regression)

Real	484.4 sec
User	134.2 sec
System	301.7 sec

3.2.3 *Validation*

Validation of the MODIS atmospheric profiles and derived parameters will be approached in several ways. Well-calibrated radiances are essential for the development of accurate algorithms. We plan to verify the MODIS infrared radiances by using collocated

data from two sensors onboard a NASA ER-2 high altitude aircraft. The MAS is a fifty channel visible, near-infrared, and thermal infrared scanning spectrometer with 50 m spatial resolution at nadir (King et al. 1996), and the HIS is a nadir-viewing Michelson interferometer with 0.5 cm^{-1} spectral resolution from 4 to 15 μm (Revercomb et al. 1988) and 2 km spatial resolution at nadir. The calibration of the HIS is such that it serves as a reference for line-by-line radiative transfer models. The MAS infrared channels are calibrated through two onboard blackbody sources that are viewed once every scan, taking into account the spectral emissivity of the blackbodies. Our first coordinated validation campaign would occur within the first year after MODIS launch, and would be a land-based field campaign with the ER-2 over the ARM CART site in Oklahoma. Data to be collected would include simultaneous ground-based CLASS-sonde temperature and moisture profiles, AERI (a ground-based Michelson interferometer) uplooking radiance spectra, tower measurements of temperature and moisture at various elevations, microwave moisture measurements, lidar and radar cloud observations, and whole sky camera images. Two field campaigns at the CART site are planned (Aug.-Sep. 1998 and Apr.-May 1999).

MODIS retrievals from the calibrated radiances will be compared to those determined from in situ radiosonde measurements, the NOAA HIRS operational retrievals, the GOES sounder operational retrievals, NCEP analysis of all available data, and retrievals from the Atmospheric Infrared Sounder (AIRS/AMSU/MHS) on the EOS PM-1 platform. Total ozone will be compared to Total Ozone Mapping Spectrometer (TOMS) measurements as well as the operational NOAA ozone estimates from HIRS. A field campaign utilizing the profiler network in the US midwest with CLASS sondes and ground based (Atmospheric Emitted Radiances Interferometer, AERI) and airborne ER-2 (High resolution Interferometer Sounder, HIS) measurements and with airborne MODIS Airborne Simulator measurements will also be initiated in the first year after launch to further validate the MODIS retrievals. Precipitable water vapor measurements will be compared to (i) radiosonde measurements over the continents, (ii) model output obtained as part of the EOS data assimilation interdisciplinary science team (Dr. Robert Atlas), and (iii) periodic differential absorption lidar measurements from the ER-2 aircraft (LASE; Dr. Ed Browell).

3.2.4 *Quality Control*

Quality control will be accomplished by manual and automatic inspection of the data and comparison to other sources of information. Automatic tests will check for physically realistic output values of temperature and moisture. Regional and global mean temperatures at 300, 500, and 700 mb will be monitored for weekly consistency; similarly dew point temperatures at 700 mb will be monitored. Global and regional precipitable water will also be tracked for spurious trends. Ozone in the polar regions will be averaged regionally and monitored for weekly consistency. Acceptable variations from week to week will be determined from the actual data.

3.2.5 *Exception Handling*

The algorithm will check the validity of input radiances using metatdata attached to the data itself, and validiity tests developed post-launch. If the required input radiance data is bad, suspect, or not available, then the algorithm will record the output products as missing for that 5×5 pixel area.

3.2.6 *Data Dependencies*

The profile retrieval algorithm requires calibrated, navigated, coregistered 1 km FOV radiances from channels 20 (3.75 μm shortwave window), 22-25 (3.96 to 4.52 μm shortwave CO_2 absorption band), 27-29 (6.72 to 8.55 μm for moisture information), 30 (9.73 μm for ozone), 31-32 (11.03 and 12.02 split window), and 33-36 (13.34, 13.64, 13.94, and 14.24 μm CO_2 absorption band channels). The MODIS Cloud Mask will be also used for cloud screening, and for surface type determination (land or sea). The MODIS viewing angle for a given FOV must be known. The NCEP global model estimates of surface temperature and pressure as well as profiles of temperature and moisture will be initially used in the calculation; as the AIRS/AMSU profiles become available, they will also be used.

3.2.7 *Output Product Description*

A single output file (MOD07) combining four products will be generated as part of the MODIS atmospheric profile retrieval algorithm; Table 4 lists the parameters and their units.

Table 4: Parameters included in products MOD30, MOD07, MOD38, MOD08

Resolution: 5 × 5 pixel, Temporal sampling: Day and Night, Restrictions: Clear Sky only

TAI time at start of scan	(seconds since 1993-1-1 00:00:00.0 0)
Geodetic Latitude	(degrees_north)
Geodetic Longitude	(degrees_east)
Solar Zenith Angle, Cell to Sun	(degrees)
Solar Azimuth Angle, Cell to Sun	(degrees)
Sensor Zenith Angle, Cell to Sensor	(degrees)
Sensor Azimuth Angle, Cell to Sensor	(degrees)
Brightness Temperature, IR Bands	(K)
Cloud Mask, First Byte	(no units)
Surface Temperature	(K)
Surface Pressure	(hPa)
Processing Flag	(no units)
Tropopause Height	(hPa)
Guess Temperature Profile	(K)
Guess Dew Point Temperature Profile	(K)
Retrieved Temperature Profile	(K)
Retrieved Dew Point Temperature Profile	(K)
Total Ozone Burden	(Dobsons)
Total Totals Index	(K)
Lifted Index	(K)
K Index	(K)
Total Column Precipitable Water Vapor, IR	(cm)
Precipitable Water Vapor Low, IR	(cm)
Precipitable Water Vapor High, IR	(cm)

Retrieval Profile Pressure Levels (hPa)

5, 10, 20, 30, 50, 70, 100, 150, 200, 250, 300, 400, 500, 620, 700, 780, 850, 920, 950, 1000

4. Assumptions

The data are assumed to be calibrated (within the instrument noise), navigated (within one FOV), and coregistered (within two tenths of a FOV). The accuracy of the retrievals will depend on the on-orbit NEΔT values in the infrared channels, estimates of which were shown in Table 2. It is assumed that high-quality global forecast model (e.g. NCEP, ECMWF, or GSFC/DAO) output or analysis fields will present for the derivation of first guess temperature and moisture profiles, since the retrieval algorithm essentially adjusts the guess just enough to fit the measured radiances.

5. References

Chesters, D., Uccellini, L. W. and W. D. Robinson, 1983: Low-level water vapor fields from the VISSR Atmospheric Sounder (VAS) "split window" channels. *J. Clim. Appl. Met.*, **22**, 725-743.

Eyre, J. R., and H. M. Woolf, 1988: Transmittance of atmospheric gases in the microwave region: a fast model. *Appl. Opt.*, **25**, 3244-3249.

____, 1992: A bias correction scheme for simulated TOVS brightness temperatures. *ECMWF Technical Memorandum 186*. 28 pp.

Fleming, H. E. and W. L. Smith, 1971: Inversion techniques for remote sensing of atmospheric temperature profiles. *Reprint from Fifth Symposium on Temperature*. Instrument Society of America, 400 Stanwix Street, Pittsburgh, Pennsylvania, 2239-2250.

Fritz, S., D. Q. Wark, H. E. Fleming, W. L. Smith, H. Jacobowitz, D. T. Hilleary, and J. C. Alishouse, 1972: Temperature sounding from satellites. *NOAA Technical Report NESS 59*. U.S. Department of Commerce, National Oceanic and Atmospheric Administration, National Environmental Satellite Service, Washington, D.C., 49 pp.

Hannon, S., L. L. Strow, and W. W. McMillan, 1996: Atmospheric Infrared Fast Transmittance Models: A Comparison of Two Approaches. Proceeding of SPIE conference 2830, Optical Spectroscopic Techniques and Instrumentation for Atmospheric and Space Research II.

Hayden, C. M., 1988: GOES-VAS simultaneous temperature-moisture retrieval algorithm. *J. Appl. Meteor.*, **27**, 705-733.

Houghton, J. T., Taylor, F. W., and C. D. Rodgers, 1984: Remote Sounding of Atmospheres. Cambridge University Press, Cambridge UK, 343 pp.

Jedlovec, G. J., 1987: Determination of atmospheric moisture structure from high resolution MAMS radiance data. Ph. D. Thesis, University of Wisconsin - Madison.

Kaplan, L. D., 1959: Inference of atmospheric structure from remote radiation measurements. *Journal of the Optical Society of America*, **49**, 1004.

King, J. I. F., 1956: The radiative heat transfer of planet earth. *Scientific Use of Earth Satellites*, University of Michigan Press, Ann Arbor, Michigan, 133-136.

King, M.D., Kaufman, Y. J., Menzel, W. P. and D. Tanré, 1992: Remote sensing of cloud, aerosol, and water vapor properties from the Moderate Resolution Imaging Spectrometer (MODIS). *IEEE Trans. Geosci. Remote Sens.*, **30**, 2-27.

____, Menzel, W. P., Grant, P. S., Myers, J. S., Arnold, G. T., Platnick, S. E., Gumley, L. E., Tsay, S. C., Moeller, C. C., Fitzgerald, M., Brown, K. S. and F. G. Osterwisch, 1996: Airborne scanning spectrometer for remote sensing of cloud, aerosol, water vapor and surface properties. *J. Atmos. Oceanic Technol.*, **13**, 777–794.

Kleespies, T. J. and L. M. McMillin, 1984: Physical retrieval of precipitable water using the split window technique. Preprints Conf. on Satellite Meteorology/Remote Sensing and Applications, AMS, Boston, 55-57.

Li., J., and H. -L. Huang, 1998: Retrieval of atmospheric profiles from satellite sounder measurements using the discrepancy principle. *Appl. Optics* (in press).

Li, J., J. P. Nelson III, T. Schmit, W. P. Menzel, C. C. Schmidt, and H. -L. Huang, 1998: Retrieval of total atmospheric ozone from GOES sounder radiance measurements with high spatial and temporal resolution. *Proceedings of SPIE*, Vol. 3501, 291-300.

Ma, X. L., Smith, W. L. and H. M. Woolf, 1984: Total ozone from NOAA satellites-a physical model for obtaining observations with high spatial resolution. *J. Climate Appl. Meteor.*, **23**, 1309-1314.

Ma, X. L., Schmit, T. J. and W. L. Smith, 1999: A non-linear physical retrieval algorithm – its application to the GOES-8/9 sounder. Accepted by *J. Appl. Meteor.*

Menzel, W. P., and J. F. W. Purdom, 1994: Introducing GOES-I: The first of a new generation of geostationary operational environmental satellites. *Bull. Amer. Meteor. Soc.*, **75**, 757-781.

Menzel, W. P., F. C. Holt, T. J. Schmit, R. M. Aune, A. J. Schreiner, G. S. Wade, and D. G. Gray, 1998. Application of the GOES-8/9 soundings to weather forecasting and nowcasting. *Bull. Amer. Meteor. Soc.*, **79**, 2059-2077.

Plokhenko, Y. and W. P. Menzel, 1999: The effects of surface reflection on estimating the vertical temperature – humidity distribution from spectral infrared measurements. Submitted to *J. Appl. Meteor*

Prabhakara, C., Conrath, B. J. and R. A. Hanel, 1970: Remote sensing of atmospheric ozone using the 9.6 μm band. *J. Atmos. Sci.*, **26**, 689-697.

Revercomb, H. E., Buijs, H. , Howell, H. B., LaPorte, D. D. , Smith, W. L. and L. A. Sromovsky,1988: Radiometric Calibration of IR Fourier Transform Spectrometers: Solution to a Problem with the High Resolution Interferometer Sounder. *Applied Optics*, **27**, 3210-3218.

Rodgers, C. D., 1976: Retrieval of atmospheric temperature and composition from remote measurements of thermal radiation. *Rev. Geophys. Space Phys.*, **14**, 609-624.

Shapiro, M. A., Krueger, A. J. and P. J. Kennedy, 1982: Nowcasting the position and intensity of jet streams using a satellite borne total ozone mapping spectrometer. *Nowcasting*, K. A. Browning (ed.), Academic Press, Inc., (London) Ltd., 137-145.

Smith, W. L., Woolf, H. M., and W. J. Jacob, 1970: A regression method for obtaining real-time temperature and geopotential height profiles from satellite spectrometer measurements and its application to Nimbus 3 "SIRS" observations. *Mon. Wea. Rev..*, **8**, 582-603.

____, Woolf, H. M., Hayden, C. M., Wark, D. Q. and L. M. McMillin, 1979: The TIROS-N operational vertical sounder. *Bull. Amer. Meteor. Soc.*, **60**, 1177-1187.

____, Suomi, V. E., Menzel, W. P., Woolf, H. M., Sromovsky, L. A., Revercomb, H. E., Hayden, C. M., Erickson, D. N. and F. R. Mosher, 1981: First sounding results from VAS-D. *Bull. Amer. Meteor. Soc.*, **62**, 232-236.

____, and F. X. Zhou, 1982: Rapid extraction of layer relative humidity, geopotential thickness, and atmospheric stability from satellite sounding radiometer data. *Appl. Opt.*, **21**, 924-928.

____, Woolf, H. M. and A. J. Schriener, 1985: Simultaneous retrieval of surface and atmospheric parameters: a physical and analytically direct approach. *Advances in Remote Sensing*, A. Deepak, H. E. Fleming, and M. T. Chahine (Eds.), ISBN 0-937194-07-7, 221-232.

____, and H. M. Woolf, 1988: A Linear Simultaneous Solution for Temperature and Absorbing Constituent Profiles from Radiance Spectra. Technical Proceedings of the

Fourth International TOVS Study Conference held in Igls, Austria 16 to 22 March 1988, W. P. Menzel Ed., 330-347.

____, 1991: Atmospheric soundings from satellites - false expectation or the key to improved weather prediction. *Jour. Roy. Meteor. Soc.*, **117**, 267-297.

____, Woolf, H. M., Nieman, S. J., and T. H. Achtor, 1993: ITPP-5 - The use of AVHRR and TIGR in TOVS Data Processing. Technical Proceedings of the Seventh International TOVS Study Conference held in Igls, Austria 10 to 16 February 1993, J. R. Eyre Ed., 443-453.

Sullivan, J., Gandin, L., Gruber, A., and W. Baker, 1993: Observation Error Statistics for NOAA-10 Temperature and Height Retrievals. *Mon. Wea. Rev.*, **121**, 2578-2587.

Twomey, S., 1977: An introduction to the mathematics of inversion in remote sensing and indirect measurements. Elsevier, New York.

Wark, D. Q., 1961: On indirect temperature soundings of the stratosphere from satellites. *J. Geophys. Res.*, **66**, 77.

____, Hilleary, D.T., Anderson, S. P., and J. C. Fisher, 1970: Nimbus satellite infrared spectrometer experiments. *IEEE. Trans. Geosci. Electron.*, **GE-8**, 264-270.